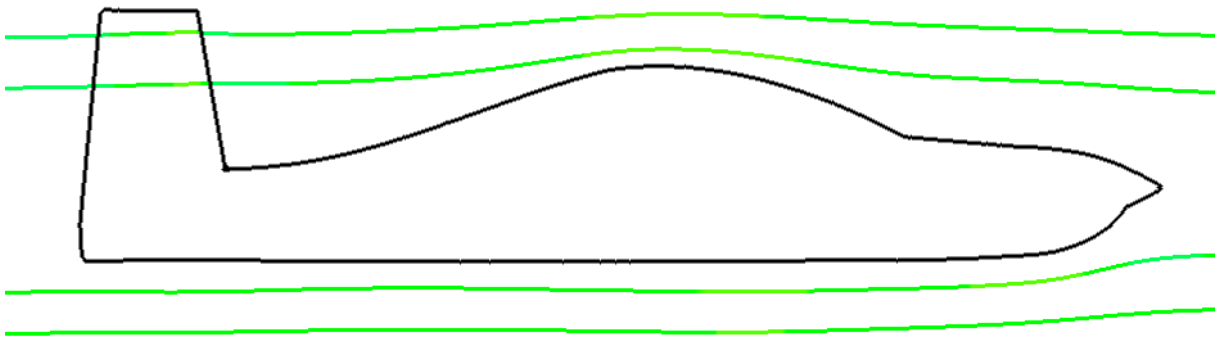


Drag Estimations on Experimental Aircraft Using CFD

Examensarbete i flygteknik 2006 (10 poäng)



Rapport av: Staffan Hardie
Rapportkod: MDH.IMA.FLY.0180.2006.C.10p.Ae

Keywords: *CFD, drag, experimental*



MÄLARDALENS HÖGSKOLA
Institutionen för matematik och fysik

Abstract

The drag approximations done in the initial design phase needed to be verified. A model of the aircraft has been analyzed with CFD and results examined to see how accurate the estimations were. A step by step analysis was made and then a simulation was run. The drag results of the CFD analysis did not meet the goal of the initial design study. Several reasons for this are discussed. The analysis shows that the aircraft design works well aerodynamically but also shows a few areas where the design can be improved.

Sammanfattning

Det approximerade värdet på luftmotståndet som gjordes i den preliminära designfasen behövde verifieras. En flygplansmodell har analyserats med CFD och resultaten har undersökts för att se hur exakta antagandena var. En analys gjordes steg för steg och slutligen har en simulering utförts. Det uppmätta luftmotståndet motsvarade inte målet i den preliminära designfasen. Flera olika anledningar till detta diskuteras. Analysen visar att denna flygplansdesign fungerar bra aerodynamiskt men identifierar också en del punkter på vilken den kan förbättras.

Preface

I would like to thank Anders Olsson for all the work he has put into this project and all the patience he has had while helping me create a suitable model for the analysis. I wish him all the best for the future of the project.

I would also like to thank my supervisor Gustaf Enebog as well as Mirko Senkovski and Sven Hugosson for their good work with the Aeronautical Engineering programme at Mälardalen University.

Helsingborg, November 15, 2006
Staffan Hardie

Table of Contents

Abstract	I
Sammanfattning	II
Preface	III
Table of Contents	IV
Abbreviations and Symbols	VI
1 Introduction	1
1.1 Background	1
1.2 Problem Definition.....	1
1.3 Purpose	1
1.4 Method	1
1.5 Results	1
2 Theory	2
3 Problem Analysis	4
3.1 The Computational Domain	4
3.2 Boundary Conditions.....	4
3.3 Discretization of the Domain	4
3.4 Initial Values	4
3.5 Convergence Criteria.....	4
3.6 Post Processing.....	4
4 Material	5
4.1 Software	5
4.2 Hardware	5
4.3 Model	5
5 Comparison Aircraft	6
5.1 Van's RV-8A.....	6
5.2 Cirrus SR20/22-G2.....	6
6 Method	7
6.1 Simulation Properties	7
6.2 Coordinate System	7
6.3 Model Properties	8
6.4 Domain Properties.....	8
6.5 Domain shape.....	9
6.6 Domain Size	10
6.7 Advantage of Symmetry.....	12
6.8 Boundary Conditions.....	12
6.8.1 Inlet.....	12
6.8.2 Outlet.....	12
6.8.3 Side Walls	12
6.8.4 Symmetry wall	13
6.8.5 Model Surface	13
6.9 Discretization of the domain	14
6.9.1 Mesh Type.....	14
6.9.2 Global Mesh	14
6.9.3 Refined Mesh	14
6.10 Initial Values	16
6.11 Convergence Criteria.....	16

7 Results	17
7.1 Computation Data	17
7.2 Convergence Check.....	17
7.3 Lift and Drag Results	18
7.4 Calculating the Drag Coefficient.....	18
7.5 Calculating the Induced Drag Coefficient.....	19
7.6 Reynolds and Mach Number.....	20
7.7 Flow Analysis.....	20
7.7.1 Recirculation Zones.....	21
7.7.2 Boundary layer	22
7.7.3 Wing Tips.....	22
8 Discussion.....	23
9 Recommendations	24
10 Bibliography	25

Abbreviations and Symbols

Alla mina ändringar (som ofta bara är förslag) är i rött. Där jag bara strykit ett ord har jag gjort det rött och understrukit så att du ser att det ”har försvunnit”

AR	Aspect ratio
AOA	Angle of attack
C_D	Drag coefficient
C_{D0}	Zero-lift drag coefficient
C_L	Lift coefficient
CFD	Computational fluid dynamics
CV	Control volume
D	Drag
D_0	Zero lift drag
D_w	Wing drag
e	Span efficiency factor
FEM	Finite element method
L	Lift
L_w	Wing lift
P	Static pressure
q_∞	Free stream dynamic pressure
S	Wing area
T	Temperature
TED	Turbulence eddy dissipation rate
TKE	Turbulence kinetic energy
V_∞	Free stream velocity
U_{vel}	Velocity along the X-axis
V_{vel}	Velocity along the Y-axis
W_{vel}	Velocity along the Z-axis
ρ	Air density
μ	Viscosity

1 Introduction

1.1 Background

A preliminary design study of a two-seater experimental aircraft for the homebuilt market has been carried out by Anders Olsson and is presented in a report with the title “Conceptual Design of Experimental Aircraft”. The study was carried out to see if it would be possible to construct an aircraft with a high cruise speed, long range, capable of aerobatics and with short field performance. During this early design phase, many assumptions were made with regards to the aircraft’s aerodynamic properties in order to make preliminary performance calculations to see if the aircraft meets the requirements.

1.2 Problem Definition

As the aircraft is taking shape, the need for a more thorough aerodynamic analysis has arisen in order to verify the assumptions made, and to see if there are any aerodynamically bad areas that need to be addressed closer. The creation of a scale model and wind tunnel tests are very costly, therefore a more theoretical approach using CFD makes sense in order to make progress with the project.

1.3 Purpose

The main purpose of the analysis is to estimate the aircraft design’s zero lift drag, C_{D0} , that is the design’s aerodynamic drag coefficient when no lift is generated by the wings. The analysis will also identify potential problem areas i.e. shapes that have adverse effects on the aerodynamic efficiency of the aircraft e.g. the fuselage-wing junction.

1.4 Method

A 3D CAD model currently exist available and will be thoroughly analyzed in a CFD program and the results will be evaluated. Initially a study will be conducted in order to determine how the simulation of the model should be performed in order to obtain the most accurate results.

1.5 Results

The results will be compared with the approximations made in the design study by Anders Olsson as well as figures for similar aircraft.

2 Theory

For many years wind tunnels have been used to study the flows of air around objects of different shapes. This has been important in order to aid the development of, for example, aircraft or to gather data on different airfoils. However, wind tunnel tests are expensive and is time consuming with tunnel size being a limiting factor when it comes to accuracy. It might not be a problem to do a test with a full scale car in a tunnel that is large enough, but aircraft are another matter due to their size. The solution is to create accurate scale models that will fit in the wind tunnel. In theory, a small model can be used to study its larger brother can it not? Yes, it can, but there are problems associated in doing so.

Air, or any other fluids for that matter, will under certain conditions flow around an object in a certain way. Velocity, size, density and viscosity are among these conditions that govern how the flow will behave. The most interesting parameter here is the size because it means that the flow will not be the same around a scale model as it will be around its real life counterpart. The object is scaled down, but the air is not.

This is where the Reynolds number comes into play. It is defined as

$$\text{Re} = \frac{\rho v L}{\mu}$$

This is the ratio between the inertial forces and the viscous forces experienced by the fluid. ρ is the density, v is the fluid's velocity, L is the characteristic length and μ is the fluid's kinematic viscosity.

This means that if a scale model is studied in a wind tunnel the other parameters would have to be adjusted to obtain the same Reynolds number, or the flow will not behave in the same way. As the model is scaled down and error corresponding to this will emerge, one solution would be to increase velocity. However as velocity increases, the Mach number will become a factor as supersonic shocks will develop. Instead of wind tunnels, water tunnels can be used since water has a different viscosity and density, in effect giving the flow a higher Reynolds number.

In the last decades, it has become more and more common to do as many of these studies as possible with the aid of CFD; this greatly reduces the time and costs as well as speeding up the projects.

The results are obtained by solving a set of equations describing the fluid flow and its boundaries. For CFD, these equations can not be solved analytically thus they have to be solved numerically to approximate the solution.

In modern CFD, the equations used are among others the Navier-Stokes equations that define the flow of basically any fluid. This is very complex and computational heavy thus require powerful computers to solve for the flow. In the past when computers were not so powerful, simplified versions of the Navier-Stokes equations were used such as the Euler equations, where viscosity is neglected. There are also several ways of modelling turbulence that are applied where this is needed.

The basics behind CFD are that you set up a control volume, CV that you want to study. There are three laws that have to be satisfied for the control volume, the conservation laws¹.

- Conservation of mass
- Conservation of momentum
- Conservation of energy

These three laws are quite easy to understand. Let us say we have a CV that is 1x1x1 cm. Any mass of fluid that enters the CV through any of its 6 boundaries also has to leave the control volume at the same rate, otherwise its mass would increase infinitely or decrease until it reaches zero. Simply put, what goes in must come out.

To be able to solve the equations for a flow accurately, the control volume needs to be split up into smaller parts, usually called elements or cells. Boundary conditions are given to the elements that are placed along the boundary of the CV and the equations are solved for each of the elements across the CV. These calculations have to be iterated several times as for any other numerical solution. When the average values of each parameter and its error converge towards a given value, the solution has converged and the results for each cell can be obtained.

¹ Blazek, J., Computational Fluid Dynamics: Principles and Applications, Second Edition , page 5

3 Problem Analysis

In order to obtain the best results possible, the CFD analysis requires careful planning. The simulation itself can take several days, or even weeks, so there will be no opportunity to re-run the simulation once it has been completed. The planning of the final simulation has been broken down into smaller steps in order to set up the analysis.

3.1 The Computational Domain

The appropriate size and shape of the computational domain, also referred to as control volume, and the best placement of the model in the domain, needs to be determined. A domain too large will make the simulation unnecessarily large and waste computational resources, however a domain too small will lower the accuracy of the results. The properties of the domain such as temperature, pressure and fluid properties need to be chosen.

3.2 Boundary Conditions

The conditions at the boundary of the domain need to be set such as inlet velocities, outlets and wall attributes.

3.3 Discretization of the Domain

Since CFD utilizes numerical solutions the domain needs to be discretized or meshed as it is more commonly referred to. The mesh will have to be refined in areas with high gradients for example close to the surface around the aircraft model.

3.4 Initial Values

Initial values need to be set for all the nodes in the domain.

3.5 Convergence Criteria

The Criteria for which the simulation can be regarded as converged needs to be determined.

3.6 Post Processing

The simulation results will give the sums of the forces acting in each direction on the model, or any chosen part of it. Through this, the drag coefficient C_D can be obtained. The amount of lift created by the wing will have to be taken into account in order to be able to calculate the induced drag. Subtracting the induced drag from the total drag should give the zero lift drag.

4 Material

4.1 Software

There are several different CFD solvers available on the market. For this analysis COSMOS DesignSTAR 3.0 with COSMOS/Flow has been chosen as this is the one available and determined to be sufficient for the analysis. COSMOS uses FEM, finite element method, for solving the flow. The modelling is done in Pro/ENGINEER Wildfire 2.0.

4.2 Hardware

The computer that will be used for the simulation is a Windows XP machine running on a Pentium D945 Dual Core 3.4 GHz CPU with 2GB RAM.

4.3 Model

A 3D model of the aircraft is available, as well as all the relevant measurements of the aircraft geometry (see Figure 4.1 and 4.2).



Figure 4.1: *Three dimensional view of the aircraft.*

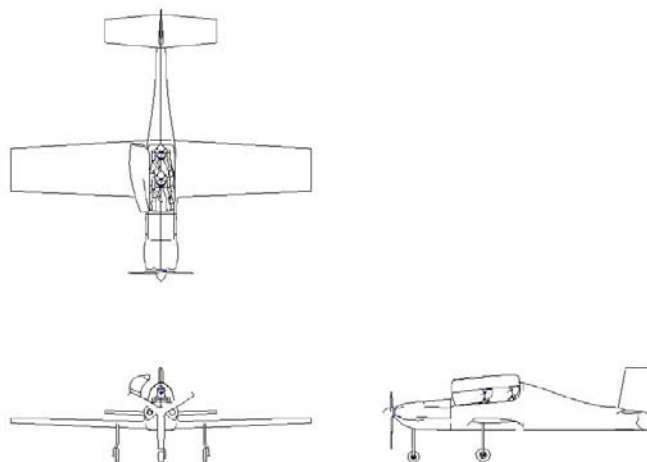


Figure 4.2: *Three view drawing.*

5 Comparison Aircraft

5.1 Van's RV-8A

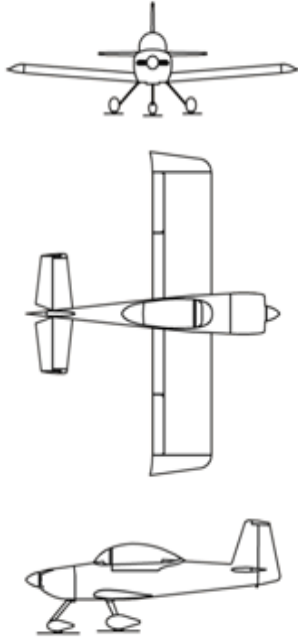


Figure 5.1: *Van's RV-8A*.

The Van's RV-8A being a tandem two-seater kit plane is the one most similar to the proposed design and is also the one used as primary comparison in the initial study.

Cruise speed: 174 kts

C_{D0} : 0.0175 (taildragger, tricycle slightly higher)

5.2 Cirrus SR20/22-G2



Figure 5.2: *Cirrus SR22-G2*.

The Cirrus SR20/22-G2 is currently one of the best selling single engine four-seat aircraft. It has a slim fuselage similar to that of the proposed design.

Cruise speed: 156 kts

C_{D0} : N/A

6 Method

6.1 Simulation Properties

The analysis will be made on a steady state, incompressible flow. The simplification of incompressible flow is very reasonable since compressibility effects for this Mach number (0.23) is low. The general consensus is that below local Mach numbers of about 0.3 compressibility effects on the fluid are small enough to be neglected. Since the model is slim, in a clean configuration and little lift generated by the wing, gradients therefore will be small and the flow will not accelerate to these high mach numbers.

The flow will be considered adiabatic meaning that there will be no heat exchange with the surrounding air. The turbulence modelling in COSMOS is done using the $K - \varepsilon$ model.

The $K - \varepsilon$ model is one of the most commonly used as it offers a reasonable compromise between computational effort and accuracy^{II}. It is based on the solution of equations for the turbulent kinetic energy K and the turbulent dissipation rate ε ^{III}.

6.2 Coordinate System

The model is placed in a Cartesian coordinate system and is oriented so that the x-axis represents the aircraft's roll axis, the y-axis represents the pitch axis and the z-axis represents the yaw axis (see Fig. 6.1).

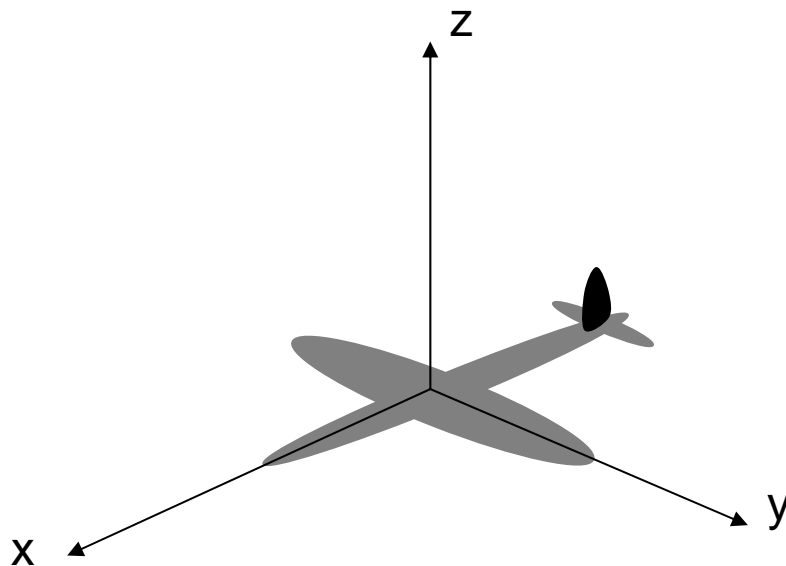


Figure 6.1: *The model's orientation in relation to the Cartesian coordinate system.*

^{II} Blazek, J., Computational Fluid Dynamics: Principles and Applications, Second Edition , page 55

^{III} Blazek, J., Computational Fluid Dynamics: Principles and Applications, Second Edition , page 243

6.3 Model Properties

The propeller and its effects will be neglected as it will make modelling too complicated and the results will be uncertain. COSMOS does not support transient analysis so an alternate model would have to be developed and verified before applying it to this study.

The air intakes for the engine cooling will be modelled as to not let any air through them, so as to simplify the analysis.

6.4 Domain Properties

The fluid velocity for the analysis was set to 82 m/s^{IV} as this was the target cruising speed of the aircraft in the conceptual study. The flow was directed to be parallel to the x-axis and in the opposite direction of it.

The fluid properties used for the analysis were the standard properties for air in COSMOS/Flow. These differ slightly from the ISA properties and will also change with increasing altitude but this has no effect on the end result as long as the same values are used when analysing the results (see Table 6.1).

The buoyancy of the fluid was ignored as the flow was incompressible and adiabatic, thus density would be constant. If the flow was not adiabatic and heat transfer with the exterior of the control volume would be present, for example a hot exhaust pipe heating the air passing it, the air would move differently because of convection caused by warmer air with lower density rising above colder denser air. This effect would be negligible when taking the velocity of the surrounding air into account.

Table 6.1: *Comparison between the standard air properties used in COSMOS and ISA standard atmosphere at sea level and at 3000 m.*

	COSMOS (standard)	ISA (sea level)	ISA (2000 m)
Pressure, P	101325 Pa	101325 Pa	79497.2 Pa
Temperature, T	293 K	288.2 K	275.15 K
Density, ρ	1.2047 kg/m ³	1.225 kg/m ³	1.00649 kg/m ³
Viscosity, μ	1.817*10 ⁻⁵ kg/ms	1.789*10 ⁻⁵ kg/ms	1.725*10 ⁻⁵ kg/ms

^{IV} Olsson, A., Conceptual Design of Experimental Aircraft, page 9

6.5 Domain shape

Several different shapes were considered for the computational domain in this study. At first a spherical domain seemed like the best solution since the distance from the model to the domain boundaries would be close to equal in all directions, meaning that the volume of the domain could be kept to a minimum (see Fig 6.2). This idea was dropped in favour for a cubical domain which was better suited for modelling and applying boundary conditions, although there would be some wasted space in the corners that would have little to no effect on the result, meaning that the computations might take a little longer than an optimal shape would. The volume of the spherical domain is only 52% of that of the cube (see Fig 6.2), although since the wasted space in the cube would not require such a fine mesh so the effect is a lot less on the computational effort required (see Chapter 6.9).

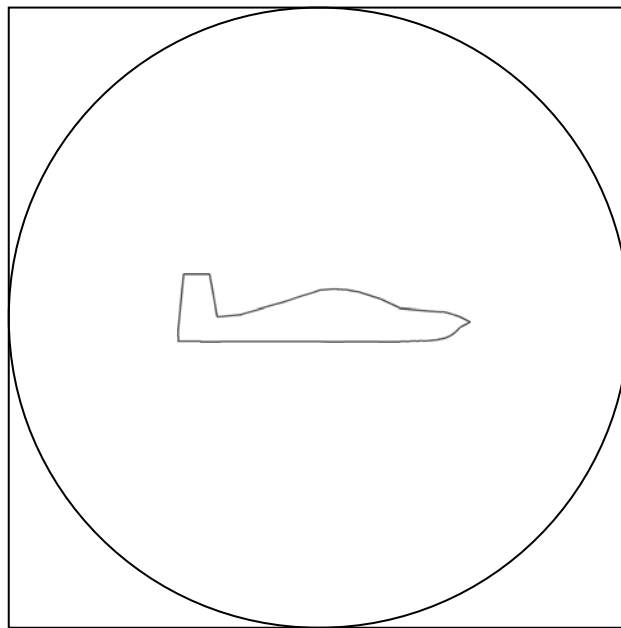


Figure 6.2: *Comparison between spherical and cubical domain.*

6.6 Domain Size

There was very little information to be found on how large a domain was required for a study such as this one, since so many different factors come into play making each case unique. However, a rough indication was that at least 10 times the model length would be required in each direction in order to obtain somewhat accurate results.

Since a too large domain would waste computational resources and a too small domain would lead to inaccurate drag estimations, a study was required to determine exactly how small a domain could be used without affecting the result.

The idea was to study how the drag of a simple geometry changed as the size of the cubical domain around it was increasing in size. The conditions would be the same as the ones in the final study with regards to velocities and fluid properties. For this study a square flat plate was considered, but in the end a cube was chosen to eliminate issues with plate thickness and the very large gradients at the edges of the plate that could affect the results. The cube with its flat surfaces allowed a slightly coarser mesh with straight edged cells to be used, significantly reducing simulation time compared to using the complex model of the aircraft. The cube is also more blunt than the aircraft so the wake will also be both longer and wider which means that it will affect the flow similarly to a larger aircraft resulting in domain slightly larger than necessary giving a bit of a safety margin for the final study. The size of the cube was chosen so that it would roughly have the same frontal area as the aircraft which was around 3 m^2 , so a cube with 1.7 meter sides was chosen.

The smallest domain chosen was $10 \times 10 \times 10 \text{ m}$ and the second smallest was $20 \times 20 \times 20 \text{ m}$ and thereafter increasing to $180 \times 180 \times 180 \text{ m}$ in steps of 20 m . In total 10 simulations were run, all meshed with roughly the same cell sizes.

The results from these simulations were plotted and the graph clearly shows how the drag curve flattens as the domain size is about $100 \times 100 \times 100 \text{ metres}$ (see Fig. 6.3). With the aircraft in the centered in the domain, it gives a domain size between ~ 46.4 and 50 metres in each direction, roughly 7 times the aircraft length of $6.88 \text{ m}^{\text{V}}$.

To be on the safe side with regards to the size, a domain which extended 60 metres from the model was chosen. It was also noted during these simulations that the wake behind the cube extended all the way to the outlet boundary so the decision was made to extend the distance behind the model to double its length, giving a domain $180 \times 120 \times 120 \text{ metres}$.

^V Olsson, A., Conceptual Design of Experimental Aircraft, page 44

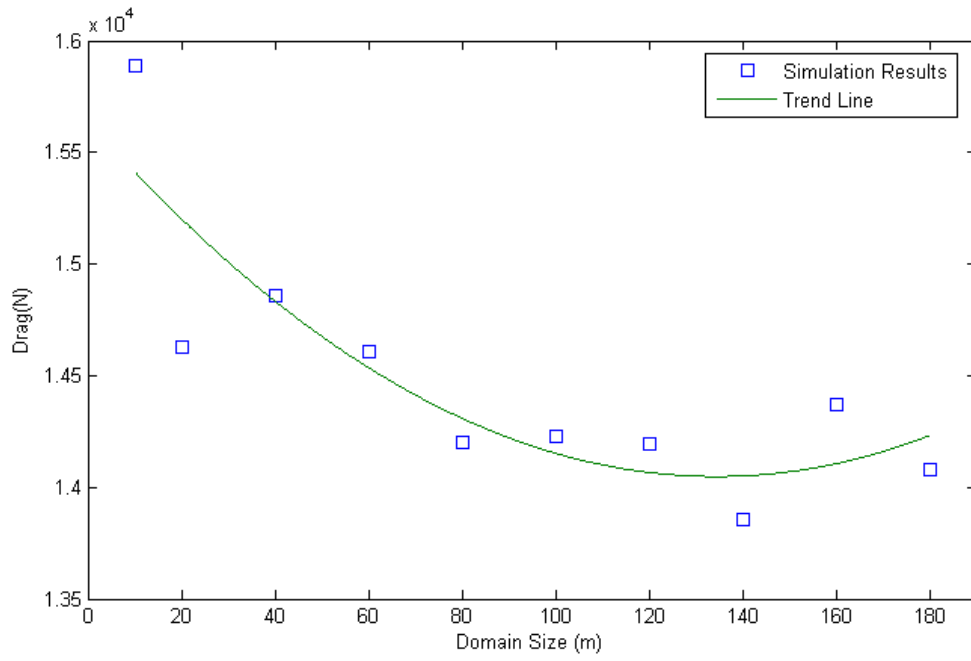


Figure 6.3: Drag reducing as domain size increases.

6.7 Advantage of Symmetry

To speed up the computations and to concentrate the computer resources, advantage will be taken of the model's symmetry. Since the model and domain is symmetric around the XZ-plane, the computations only need to be carried out on one half of the domain, since the other half will yield exactly the same, but mirrored, results. This way, the amount of elements needed can be halved and thus cutting computation time by half.

Symmetry was also used in the domain size study where the cube and its domain were symmetric around both the XY- and XZ-plane, reducing the size of the domain to one quarter of its original size.

6.8 Boundary Conditions

The domain has 5 different types of boundaries surrounding it (see Fig. 6.4 and 6.5).

- 1 Inlet (1)
- Outlet (1)
- Side walls (3)
- Symmetry wall (1)
- Model surface

6.8.1 Inlet

At the inlet, the boundary condition was set to a velocity of 82 m/s, normal to the inlet simulating the freestream. This would give a flow parallel to the longitudinal X-axis of the model.

6.8.2 Outlet

At the outlet boundary the total pressure was set to 0 as COSMOS regards this as the difference from the reference pressure. This means that the air leaving the control volume will not experience any resistance nor will it be drawn out making its velocity higher than normal.

6.8.3 Side Walls

Initially the side wall boundaries were set as velocities equal to the inlet boundary. The idea was to speed up convergence and it worked well for smaller domains. This however led to problems as the domain grew larger, causing the solution to diverge. The boundary was then changed to a slip wall. The slip wall is a friction-less wall which only has the function to stop fluid passing through it. The reason this was used was because it would have the least effect on the flow around the model. This worked better although the solution did not converge as rapidly.

6.8.4 Symmetry wall

The wall where the domain was split into two equal halves was set to slip wall, the same as the side walls.

6.8.5 Model Surface

The surface of the model was set as a no-slip wall resulting in zero velocity at the node on the wall, letting a boundary layer form in the adjacent nodes as the computations progressed. This would give the right friction forces the flow exerts on the model.

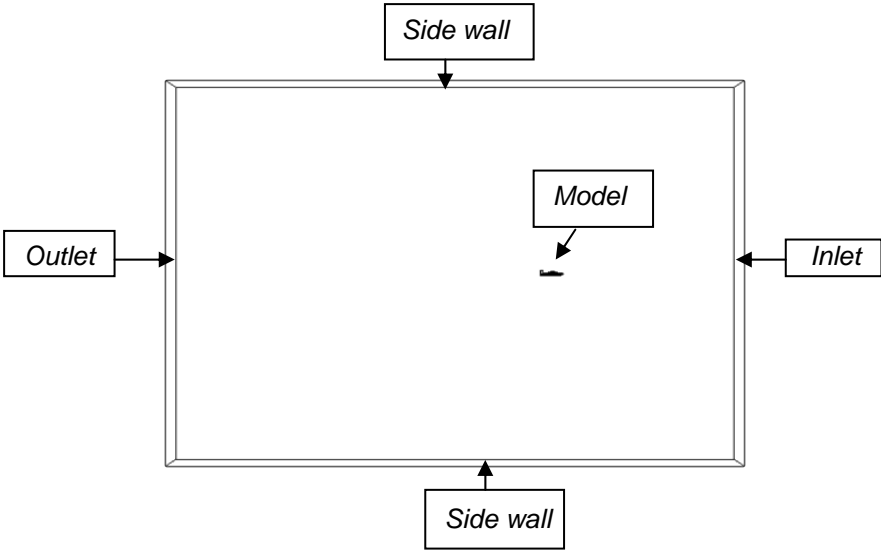


Figure 6.4: The domain with its boundaries seen from the symmetry wall.

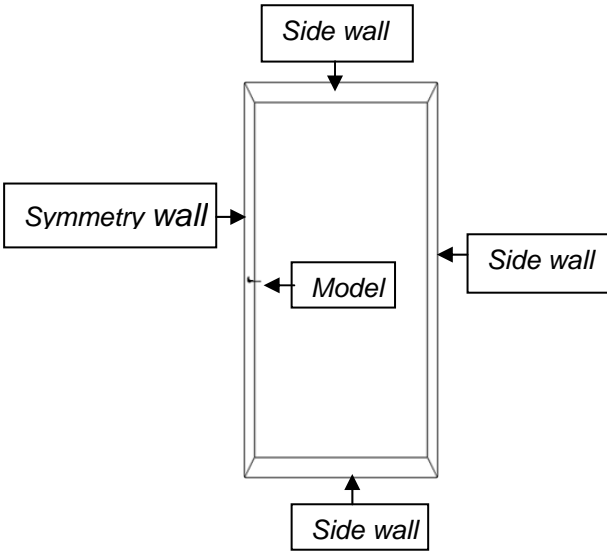


Figure 6.5: The domain with its boundaries seen from the inlet.

6.9 Discretization of the domain

To speed up computations the mesh used was coarser in areas with very small gradients, where the model has very little effect on the flow, such as at the far boundaries. With the same logic, the mesh was made finer along the model surface with high gradients, such as leading edges where the flow takes a sharp turn around the model. The way this is done in COSMOS is by setting a global element size and using mesh control to refine the mesh around chosen surfaces.

6.9.1 Mesh Type

The mesh used by COSMOS is an unstructured grid with tetrahedral elements. The high quality mesh option that was used for this analysis allows for the elements to have parabolic sides, which makes meshing around curved surfaces easier. This feature is perfect for meshing around airfoils such as the one analyzed here. Normal tetrahedral elements have 1 node in each corner, resulting in 4 nodes per element. The parabolic elements have another 6 nodes, one on each edge of the element, giving a total of 10 nodes per element (see Fig. 6.6).

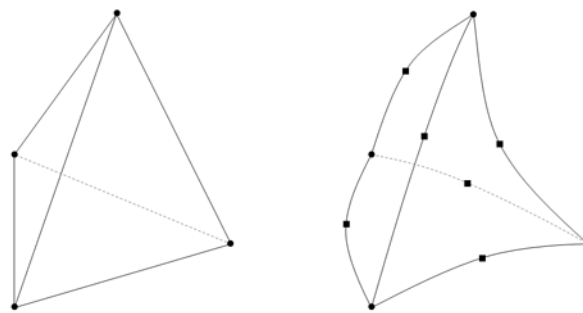


Figure 6.6: *Standard tetrahedral element and parabolic tetrahedral element with additional nodes.*

6.9.2 Global Mesh

The global mesh defines the element size in any part of the domain where the element size has not actively been reduced through mesh control. The global element size chosen was 5 metres with a tolerance of 1.5 cm. This value was chosen because it was determined to be a good balance between element size and element count. Smaller elements would have greatly increased the element count while not improving results.

6.9.3 Refined Mesh

The mesh around the model was refined so that the smallest element size was 0.05 m. The element growth ratio was set to 1.2. The thickness of the refined mesh was about 30 layers, which was adequate for letting the refined mesh grow to the global size. A smaller element size at the surface would have been desirable, but the computer's hardware became a limiting factor. When the meshing was finished, the final mesh consisted of 397,259 elements and 563,354 nodes (see Fig. 6.7 and 6.8).

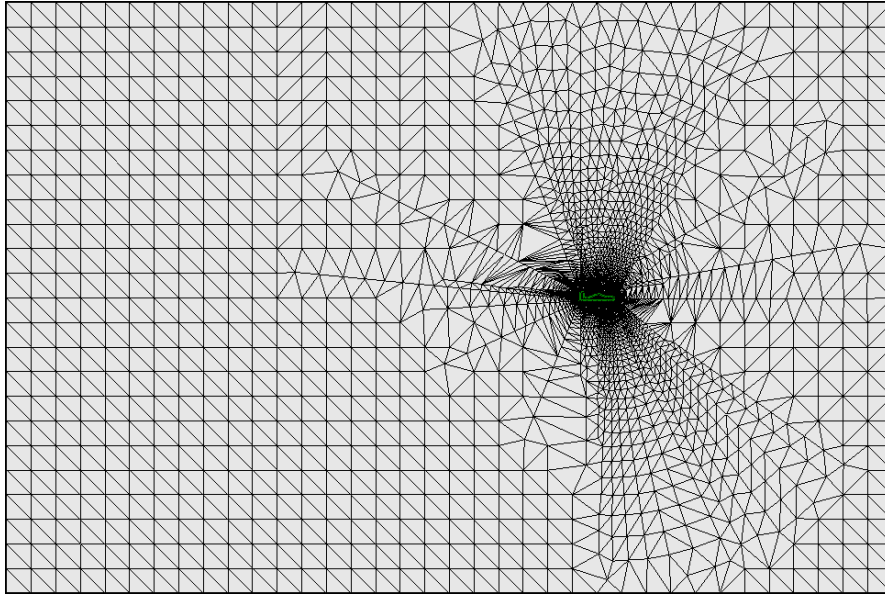


Figure 6.7: *The finished mesh along the symmetry plane with the model contour highlighted in green.*

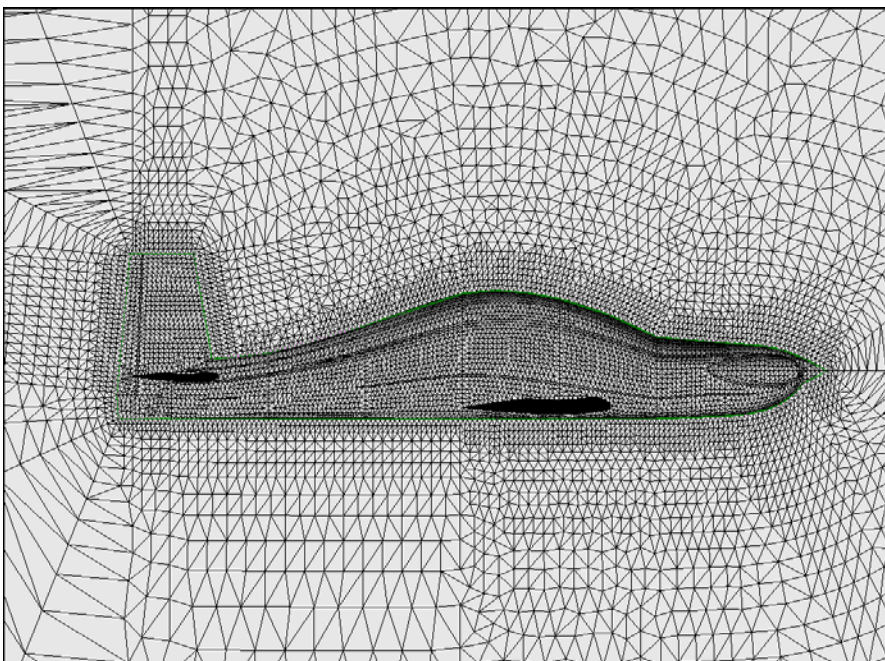


Figure 6.8: *The refined mesh around the model in the symmetry plane, with the model contour highlighted in green.*

6.10 Initial Values

Initial values are automatically set by COSMOS, based on the boundaries and the free stream conditions.

6.11 Convergence Criteria

When the simulation parameters and their residuals changed with less than 0.1% between iterations, the solution was considered converged. COSMOS does not have the feature to run the simulation until the criteria is met, meaning it would be difficult to get this spot on, so a set amount of iterations would have to be run and then checked for convergence.

7 Results

7.1 Computation Data

2,500 iterations were run, in stages of 500. Each stage took about 40 hours to complete meaning that the effective time of the complete simulation was about 8 days.

7.2 Convergence Check

At 2,000 iterations, all graphs for the flow parameters were levelling out and a quick check showed that the analysis still had some way to go. 500 more iterations were made and the convergence check looked much better.

Table 7.1: Convergence check after iteration 2000. Values outside limits in bold.

	#1999	#2000	<i>difference</i>	<i>% difference</i>
U _{vel} average	-76.289	-76.290	-0.001	0.0013
U _{vel} residual	17.312	17.243	-0.069	-0.3986
V _{vel} average	-0.664	-0.664	-0.000042	0.0063
V _{vel} residual	6.217	6.202	-0.015	-0.2461
W _{vel} average	-0.776	-0.776	-0.000083	0.0107
W _{vel} residual	12.422	12.371	-0.051	-0.4106
P average	-4229.9	-4229.9	0	0
P residual	0	0	0	0
TKE average	60.817	60.816	-0.010	-0.0016
TKE residual	51.970	51.820	-0.150	-0.2886
TDE average	1720.5	1720.6	0.1	0.0058
TDE residual	123.59	136.20	12.61	10.2031

Table 7.2: Convergence check after iteration 2500. Values outside limits in bold.

	#2499	#2500	<i>difference</i>	<i>% difference</i>
U _{vel} average	-76.415	-76.415	0	0
U _{vel} residual	4.630	4.575	-0.0548	-1.184
V _{vel} average	-0.669	-0.669	-0.000009	0.0013
V _{vel} residual	1.7637	1.7637	0	0
W _{vel} average	-0.786	-0.786	-0.000001	0.0001
W _{vel} residual	2.694	2.621	-0.0734	-2.724
P average	-4228.6	-4228.6	0	0
P residual	0	0	0	0
TKE average	60.518	60.518	0	0
TKE residual	13.094	13.043	-0.051	-0.3895
TDE average	1723,2	1723,2	0	0
TDE residual	120.33	119.66	-0.67	-0.5568

As can be seen in table 7.2, the average values were changing with less than 0.1% between iterations but the residuals were not within the limit. Investigating this further showed that the residual terms were oscillating with constant amplitude, which means that as the residual term itself got smaller, the difference in percent would grow larger. The solution is therefore considered converged.

7.3 Lift and Drag Results

The sums of the forces acting on the entire model are displayed below in their Cartesian components.

$$\begin{array}{lll} F_X & -4\,548.6 \text{ N} & \text{Total drag, } D \\ F_Y & 0 \text{ N} & \\ F_Z & 5\,202.4 \text{ N} & \text{Total lift, } L \end{array}$$

Below are results for the wing only.

$$\begin{array}{lll} F_X & -2\,746.8 \text{ N} & \text{Wing drag, } D_w \\ F_Y & 0 \text{ N} & \\ F_Z & 4\,191.4 \text{ N} & \text{Wing lift, } L_w \end{array}$$

These results show that the wing accounts for 60% of the total drag and 81% of the generated lift at a zero degree pitch angle.

7.4 Calculating the Drag Coefficient

The drag coefficient is defined as

$$C_D = \frac{D}{q_\infty S} \quad \text{VI}$$

Where q_∞ is the free stream dynamic pressure and S is the wing area.

$$C_D = \frac{4548.6}{4050.2 * 11.2}$$

$$C_D = 0.0999$$

^{VI} Anderson, J., Fundamentals of Aerodynamics, Third edition, page 20

7.5 Calculating the Induced Drag Coefficient

The total drag obtained in the analysis result can be split up into two parts, the zero lift drag and the induced drag.

$$C_D = C_{D0} + C_{Di} \quad \text{VII}$$

Zero lift drag can be rewritten as

$$C_{Di} = \frac{C_L^2}{\pi e AR} \quad \text{VIII}$$

Where C_L is the lift coefficient, e is the span efficiency factor and AR is the wing aspect ratio.

$$C_L = \frac{L}{q_\infty S} \quad \text{IX}$$

Where q_∞ is the free stream dynamic pressure and S is the wing area.

$$q_\infty = \frac{1}{2} \rho_\infty V_\infty^2 \quad \text{X}$$

$$C_L = \frac{4191.4}{4050.2 * 11.2}$$

$$C_L = 0.0921$$

$$C_{Di} = \frac{0.0921^2}{4050.2 * 11.2}$$

$$C_{Di} = 0.000529$$

This gives us the zero lift drag coefficient

$$C_{D0} = C_D - C_{Di}$$

$$C_{D0} = 0.0999 - 0.000529$$

$$C_{D0} = 0.0994$$

^{VII} Anderson, J., Fundamentals of Aerodynamics, Third edition, equation 5.4, page 356

^{VIII} Anderson, J., Fundamentals of Aerodynamics, Third edition, equation 5.62, page 374

^{IX} Anderson, J., Fundamentals of Aerodynamics, Third edition, page 20

^X Anderson, J., Fundamentals of Aerodynamics, Third edition, page 20

7.6 Reynolds and Mach Number

The Reynolds number for the flow simulated is 7 457 000 based on average chord length and the Mach number at the inlet is 0.238967.

7.7 Flow Analysis

The flow around the model in terms of the velocity is shown in Figure 7.1. It displays the magnitude of the velocity in the symmetry plane and clearly shows the accelerated flow around the canopy and around the engine cowling, as well as the flow slowing down at the trailing edge of the vertical fin and in its wake. As can be seen on the scale, the maximum velocity is 131 m/s which is almost 60% higher than the free flow velocity and gives a local Mach number of 0.38. Even though this is above the limit for where a flow can be treated as incompressible it probably has little effect on the results as it is only a small area on the forward portion of the wing that is experiencing a Mach number higher than 0.3.

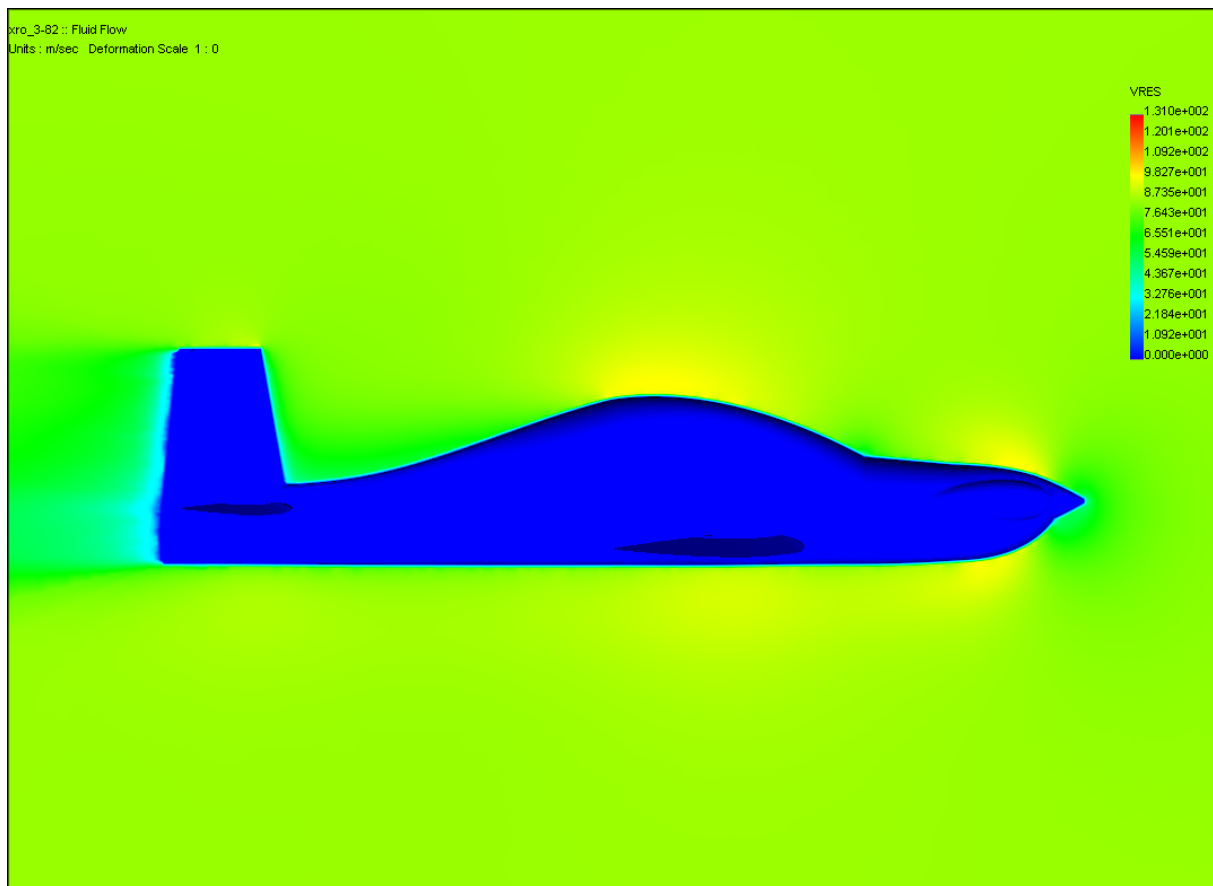


Figure 7.1: *The magnitude of the velocity in the symmetry plane.*

7.7.1 Recirculation Zones

The first step is to make a closer examination of the flow to look for recirculation zones. This is where flow has separated and is turning in the wrong direction. This will generally happen over a stalled wing or where the flow has to take a sharp turn, for example around a very blunt object. The importance in identifying and eliminating recirculation zones is due to the fact that they indicate pressure drag, which has a comparably greater magnitude than the friction drag. An aerodynamically slim design such as an aircraft fuselage should have no recirculation zones whilst in normal flight.

Upon examining the results, one recirculation zone is found at the root of the horizontal stabilizer where it meets the vertical fin (see Fig. 7.2). It is a very small zone, only a few centimetres in size and is probably due to interference between the horizontal and vertical stabilizer that are placed very close together. A smoother transition or simply separating them can solve this.

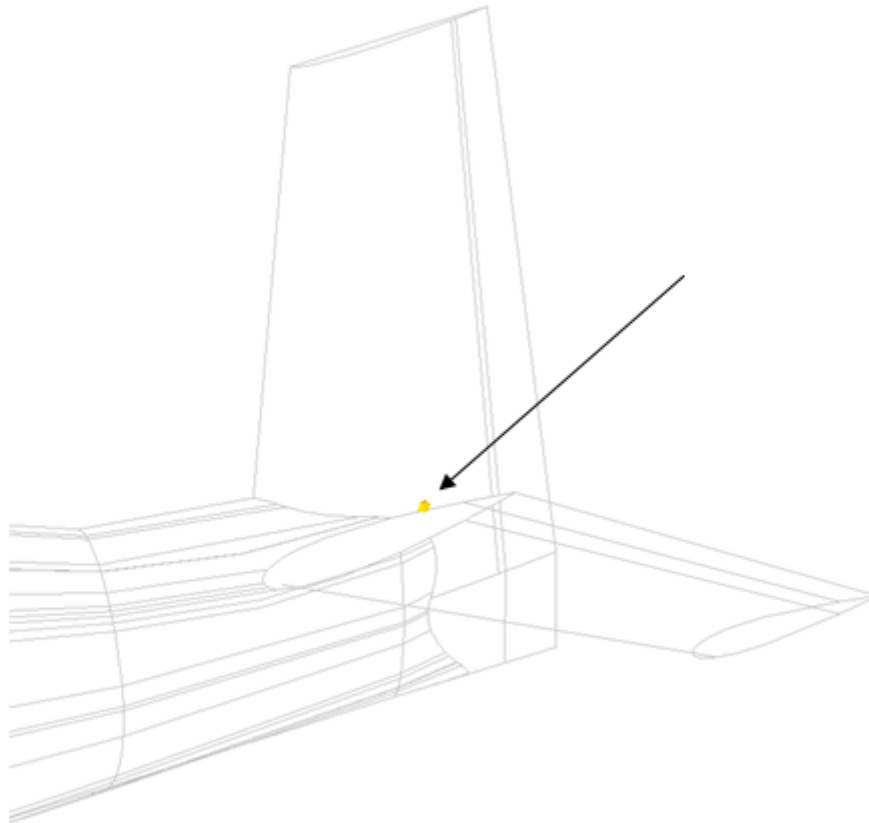


Figure 7.2: *Recirculation zone on the stabilizer.*

7.7.2 Boundary layer

Examination of the boundary layer can give useful information about the quality of the design. A nice smooth boundary layer with no rapid changes is desirable. The simulation results show a slightly jagged boundary layer around many parts of the model where a smooth layer was to be expected, for instance around the canopy and below the belly (see Fig. 7.3). This can be either due to the boundary layer being turbulent or to inadequate meshing.

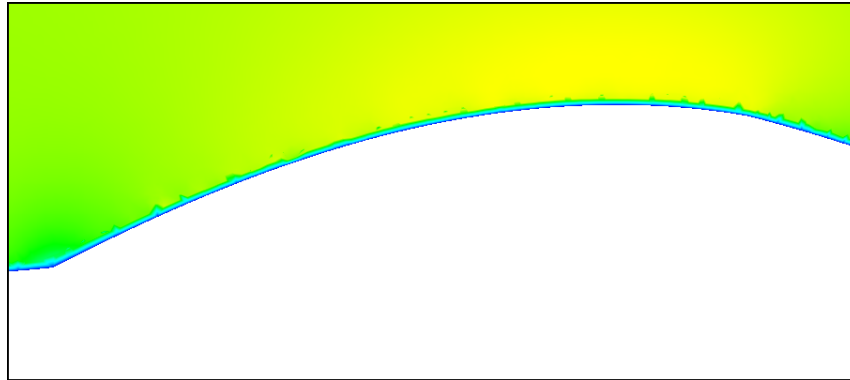


Figure 7.3: *Boundary layer above the canopy.*

7.7.3 Wing Tips

At the tips of the wings and stabilizers there is a slight increase in velocity as the air is sucked around the tip as seen in the top right of the figure (see Fig. 7.4). The flow is not separating but there is an area of low pressure increasing drag. Rounding off the leading edge towards the tip might solve this.

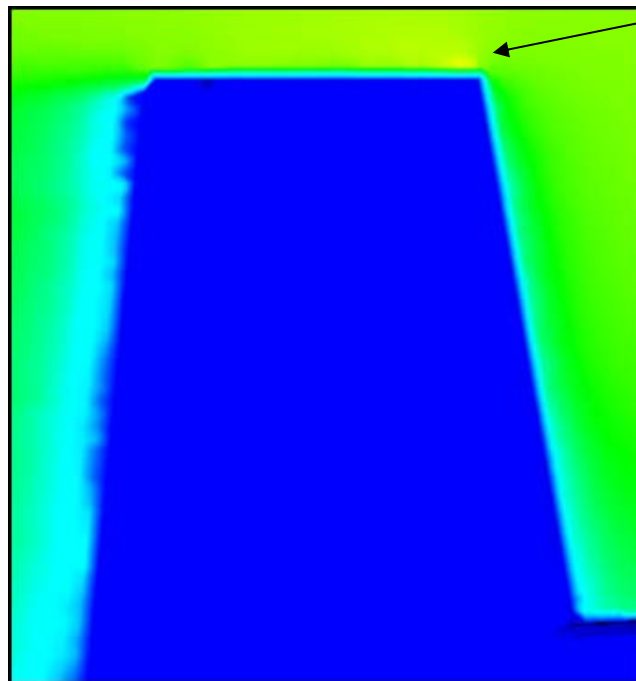


Figure 7.4: *Pressure drag at the tip of the vertical stabilizer.*

8 Discussion

The number for the zero lift drag that was approximated in the initial study was 0.0165. Although this is a low number, it should be achievable with a slim tandem design with a clean exterior. Considering the RV-8A has a C_{D0} of 0.0175 with fixed gear and a sheet metal riveted fuselage, a slim design with a composite fuselage and retractable gear should easily be more efficient. The number given by this CFD analysis is 0.0994 which is obviously too high as small single engine propeller aircraft are usually around 0.025 and vary up to about 0.03. Supersonic aircraft usually have a drag coefficient similar to the one obtained through this study which clearly shows that it cannot be an accurate result.

This inaccurate result can have several explanations. The first thing that comes to mind when examining the plots of the results is that the element sizes in the close proximity of the aircraft body are too large. This is showing up as an uneven boundary layer that is jagged and coincides with the elements. Setting another level of control with a much finer mesh, with a thickness sufficient to cover the boundary layer, might be a way to improve accuracy. Some CFD solvers allow the user to run the simulation and refine the mesh in areas with higher gradients, however, COSMOS does not permit this which makes it difficult to mesh as the refined mesh has to be adjacent to a surface of the model.

Errors when the model was imported into COSMOS might also have had its effects on the result, as the plots of the surface pressure on the model clearly show some of the joints between the surfaces in the model that were not visible in the model before running the simulation. (see Fig 8.1).

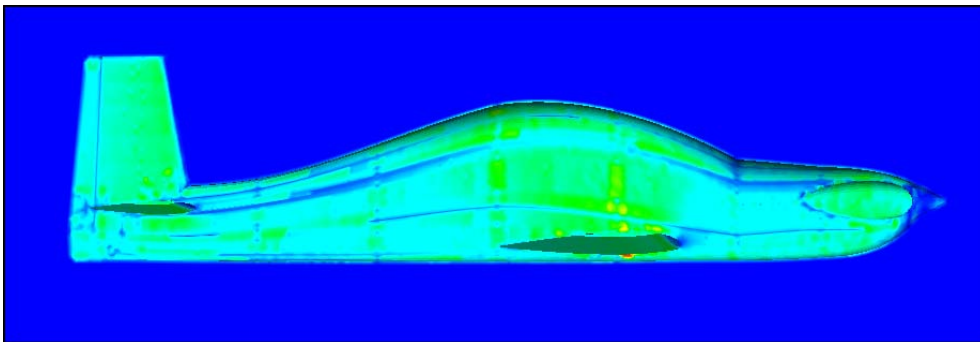


Figure 8.1: *Resultant fluid force on the model surface.*

All in all, the flow around the aircraft looks good. There are no large pressure gradients that will have adverse drag effects on the body.

9 Recommendations

The results from the analysis show that the total lift generated by the wing is not sufficient to counteract the aircraft's weight. It is recommended that the angle of incidence for the wing is adjusted in order to generate the desired lift in level flight.

Rounding off the leading edges of wings and stabilizers towards the tip should decrease drag slightly. The comparison aircraft ^{XI} Van's RV-8A and Cirrus SR20 both have rounded tips (see Figure 5.1 and 5.2).

^{XI} Olsson, A., Conceptual Design of Experimental Aircraft, page 9

10 Bibliography

Anderson, John D., Fundamentals of Aerodynamics, Third Edition (2001)

Blazek, J., Computational Fluid Dynamics: Principles and Applications, Second Edition (2005)

Olsson, Anders, Conceptual Design of Experimental Aircraft (2006)

Images from the web

Figure 5.2: <http://www.cirrusdesign.com/aircraft/gallery/srg2/22G2sunset.jpg>